Pergamon

Carbon Vol. 36, No. 9, pp. 1337–1345, 1998
© 1998 Elsevier Science Ltd
Printed in Great Britain. All rights reserved
0008-6223/98 $19.00 + 0.00

PII: S0008-6223(98)00115-8

OZONE TREATMENT OF CARBON FIBER FOR REINFORCING CEMENT

XULI FU, WEIMING LU and D. D. L. CHUNG*
Composite Materials Research Laboratory, State University of New York at Buffalo, Buffalo, NY 14260-4400, U.S.A.

(*Received* 22 *September* 1997; *accepted in revised form* 20 *February* 1998)

Abstract—Ozone treatment of isotropic-pitch-based carbon fiber was found to increase the surface oxygen concentration and change surface oxygen from C–O to C=O, thereby causing the contact angle between fiber and water to be decreased to zero. Thus, the bond strength between fiber and cement paste was increased and the tensile strength, modulus and ductility of carbon fiber reinforced cement paste were increased. Moreover, the degree of dispersion of fibers in mortar was increased and the effectiveness of the fibers for reducing the drying shrinkage was improved. As a consequence, the strain sensing ability of carbon fiber reinforced mortar was improved in terms of increased gage factor and better repeatability. The ozone treatment did not affect the morphology, tensile strength or volume electrical resistivity of the fiber itself. © 1998 Elsevier Science Ltd. All rights reserved.

Key Words—A. Carbon composites, A. carbon fibers, B. oxidation, D. mechanical properties, D. electrical properties.

1. INTRODUCTION

Short carbon fibers are used in concrete for increasing the tensile and flexural strengths, increasing the tensile ductility and flexural toughness, decreasing the drying shrinkage and rendering the concrete the ability to sense its own strain [1–25].

Surface treatment of carbon fibers is widely used for enhancing the bond between fibers and the matrix in a composite [26]. Due to the wide usage of carbon fibers in polymer–matrix composites, most surface treatments have been developed for polymer matrices, particularly epoxy [27–34]. Little attention has been previously given to the surface treatment of carbon fibers for the cement matrix [35,36], even though the bond between fiber and matrix is weaker for the cement matrix than for polymer matrices. Due to the necessity for low cost for any material used in concrete, the carbon fibers used for reinforcing concrete need to be general-purpose short fibers, most commonly those made from isotropic pitch. Thus, this paper is focused on the surface treatment of isotropic-pitch-based carbon fibers, in contrast to the previous surface treatment work conducted on high-performance carbon fibers for polymer matrices.

The most common surface treatment of carbon fibers in previous work involves oxidation, whereby oxygen-containing functional groups are formed on the surface of the fibers. The oxidation can be achieved by heat treatment in air, oxygen (O_2) or ozone (O_3) [37], chemical (e.g. nitric acid) treatment, anodic oxidation, plasma treatment, etc. In this work, by oxidation using ozone at 160°C, we have greatly improved the effectiveness of carbon fibers for reinforcing cement. In addition, the strain sensing ability of carbon fiber reinforced cement was improved by the ozone treatment. This paper covers the ozone treatment and its effects on fiber and composite properties. The fiber properties addressed are the volume electrical resistivity, tensile strength, wettability by water, surface composition, morphology, bond strength with cement and contact electrical resistivity with cement. The composite properties addressed are the volume electrical resistivity (related to the degree of fiber dispersion), drying shrinkage (related to the fiber–matrix bond strength), tensile strength, modulus and ductility, and strain sensing ability.

2. EXPERIMENTAL METHODS

The carbon fibers were isotropic-pitch-based and unsized, as obtained from Ashland Petroleum Co. (Ashland, KY). The fiber properties are shown in Table 1. As-received and five types of surface treated fibers were used. The surface treatments included immersion (with stirring) of the fibers at room temperature for 24 hours in acetic acid (99.9% reagent, 2N), H_2O_2 (31.2% reagent, 2N), NaOH solution (98.4% reagent, 1.5N) or nitric acid (60% reagent,

Table 1. Properties of carbon fibers

Filament diameter	15 ± 3 μm
Tensile strength	690 MPa
Tensile modulus	48 GPa
Elongation at break	1.4%
Electrical resistivity	3.0×10^{-3} V·cm
Specific gravity	1.6 g cm^{-3}
Carbon content	98 wt%

*Corresponding author. Tel: +1 716 645 2593 ext 2243; Fax: +1 716 645 3875.

1.5N) (followed by water washing at room temperature and air drying at 110°C) and exposure of the fibers to O_3 gas (0.6 vol%, in O_2) for 5 minutes at 160°C. Prior to O_3 exposure, the fibers had been dried at 110°C in air for 1 hour.

Cement paste made from Portland cement (Type 1) from Lafarge Corp. (Southfield, MI) was used for the cementitious material. Five types of pastes were used, namely: (i) plain cement paste (with only cement and water, such that the water/cement ratio = 0.45); (ii) cement paste with fibers (together with water reducing agent in the amount of 1 wt% of cement and with the water/cement ratio = 0.32); (iii) cement paste with fibers and methylcellulose in the amount of 0.4 wt% of cement (together with water reducing agent in the amount of 1 wt% of cement, and with the water/cement ratio = 0.32); (iv) cement paste with fibers, methylcellulose in the amount of 0.4 wt% of cement and silica fume (#965, Elkem Materials Inc., Pittsburgh, PA) in the amount of 15 wt% of cement (together with water reducing agent in the amount of 3 wt% of cement, and with the water/cement ratio = 0.35); and (v) cement paste with fibers and latex in the amount of 20 wt% of cement (water/cement ratio = 0.23, without water reducing agent). Methylcellulose, silica fume and latex serve to help the fiber dispersion [38]. The combined use of silica fume (average particle size 0.15 mm; particle size range 0.03–0.5 mm; 94% SiO_2) and methylcellulose (a surfactant), as in paste (iv), is particularly effective [38,39]. Fibers were in the amount of 0.5 wt% of cement (or 0.51 vol%). The water reducing agent used was TAMOL SN (Rohm and Haas Co., Philadelphia, PA), which contained 93–96% sodium salt of a condensed naphthalenesulfonic acid. The methylcellulose used was Dow Chemical, Midland, MI, Methocel A15-LV. The defoamer (Colloids Inc., Marietta, GA, 1010) used whenever methylcellulose was used was in the amount of 0.13 vol%. The latex (Dow Chemical, Midland, MI, 460NA) used was a styrene–butadiene polymer. The antifoam (Dow Corning, Midland, MI, 2210) used whenever latex was used was in the amount of 0.5% of the weight of the latex.

A Hobart mixer with a flat beater was used for mixing. For the case of cement paste containing latex, the latex and antifoam first were mixed by hand for about 1 minute. Then this mixture, cement, water and the water reducing agent were mixed in the mixer for 5 minutes. For the case of cement paste containing methylcellulose, methylcellulose was dissolved in water and then the defoamer was added and stirred by hand for about 2 minutes. Then this mixture, cement, water, water reducing agent and silica fume (if applicable) were mixed in the mixer for 5 minutes. After pouring the mix into oiled molds, a vibrator was used to decrease the amount of air bubbles. The specimens were demolded after one day and then allowed to cure at room temperature in air (40% relative humidity) for 28 days.

The contact electrical resistivity between the fiber and the cement paste was measured at 28 days of curing using the four-probe method with silver paint as electrical contacts, as illustrated in Fig. 1. One current contact and one voltage contact were on the fiber, while the other voltage and current contacts were on the cement paste embedding the fiber to a distance ranging from 0.51 to 1.20 mm, as measured for each specimen. The fiber diameter was in the range 15 ± 3 mm, as measured for each specimen by scanning electron microscopy after testing. The cement paste thickness was 1 mm on each side sandwiching the fiber. The fiber length was 1 cm. The resistance between the two voltage probes was measured by using a Keithley 2001 multimeter; it corresponds to the sum of the fiber volume resistance, the interface contact resistance and the cement paste volume resistance. The measured resistance turned out to be dominated by the contact resistance, to the extent that the two volume resistance terms can be neglected. The contact resistivity (in $V \cdot cm^2$) is given by the product of the contact resistance (in V) and the contact (interface) area (in cm^2), such that the contact area depends on the embedment length of the particular specimen.

Single fiber pull-out testing was conducted on the same interface samples and at the same time as the contact resistivity was measured. For pull-out testing, one end of the fiber was embedded in cement paste, as in Fig. 1. A Sintech 2/D screw-action mechanical testing system was used. The contact resistivity was taken as the value prior to pull-out testing. The bond strength was taken as the maximum shear stress during pull-out testing. Figure 2 gives typical plots of shear stress vs displacement and of contact resistivity vs displacement simultaneously obtained during pull-out testing.

Dog-bone shaped specimens of the dimensions shown in Fig. 3 were used for tensile testing of cement pastes, in addition to testing their tensile strain

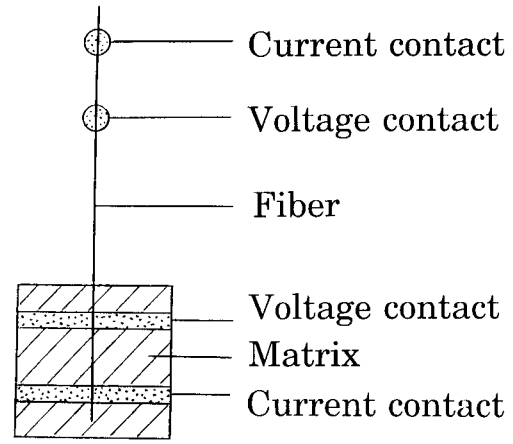

Fig. 1. Sample configuration for measuring the contact electrical resistivity of the interface between a fiber and cement paste.

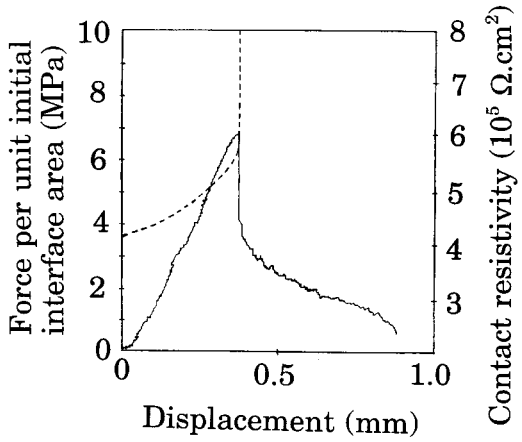

Fig. 2. Plots of shear stress vs displacement (solid curve) and of contact electrical resistivity vs displacement (dashed curve) simultaneously obtained during pull-out testing of as-received carbon fiber from cement paste at 28 days of curing.

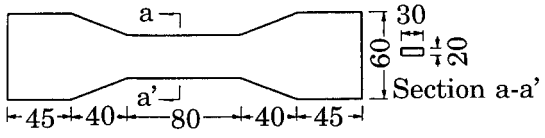

Fig. 3. Shape and dimensions (in mm) of the specimens tested under tension.

sensing ability under cyclic loading within the elastic regime. For tensile strain sensing ability testing, only cement paste (iv) was used. For conventional tensile testing, all of pastes (i)–(v) were used. The specimens were prepared by using molds of the same shape and size. Tensile testing was performed using a screw type mechanical testing system (Sintech 2/D). The displacement rate was 1.27 mm min^{-1}. The tensile strain was measured by a strain gage. Six specimens of each composition were tested.

Mortar rather than cement paste was used for testing the volume electrical resistivity, the drying shrinkage and the compressive strain sensing ability. Fibers in the amount of 0.5 wt% of cement (corresponding to 0.24 vol% of mortar) were used. The sample preparation of mortar was the same as that of cement paste (iv), except that sand was added together with silica fume. The sand was natural sand, the particle size analysis of which is shown in Fig. 1 of ref. [20]. The sand/cement ratio was 1.0. No large aggregate was used. The slump was 130 mm.

The volume electrical resistivity was measured by the four-probe method, using silver paint for the electrical contacts. The specimen size was $160 \times 40 \times 40$ mm^3. Six specimens of each type were tested.

The drying shrinkage was investigated by measuring the length change in accordance with ASTM C490-83a. The specimen size was $25.4 \times 25.4 \times 286$ mm^3 ($1 \times 1 \times 11.25$ in^3). The accuracy in the length change measurement was ± 0.0025 mm (0.0001 in.).

The strain sensing ability was tested under tension (using cement pastes) and compression (using mortars). Simultaneous to mechanical testing, DC electrical resistance measurements were made. For compressive testing according to ASTM C109-80, specimens were prepared by using a $2 \times 2 \times 2$ in^3 ($5.1 \times 5.1 \times 5.1$ cm^3) mold. The compressive strain was measured by the crosshead displacement, while the fractional change in electrical resistance along the stress axis was measured using the four-probe method. The electrical contacts were made by silver paint. Although the spacing between the contacts changed upon deformation, the change was so small that the measured resistance remained essentially proportional to the resistivity. Testing was performed under cyclic loading within the elastic regime. A hydraulic mechanical testing system (MTS Model 810) was used for compressive testing.

The dynamic contact angle between carbon fiber and deionized water was measured using the Sigma 70 tensiometer of KSV Instruments (Monroe, CT). The tensiometric method (micro-Wilhemy technique) was used. The immersion depth was up to 3 mm and the stage with a beaker of water was moved up (advancing) and down (receding) at a constant speed of 3 mm min^{-1}. Five samples of each type were tested.

The surface composition of carbon fiber was measured by ESCA. The surface morphology before and after pull-out of a single fiber from cement paste was examined by scanning electron microscopy (SEM). The volume electrical resistivity of a single fiber was measured by the four-probe method, using silver paint for electrical contacts. The tensile strength of a single fiber was measured by using a Sintech 2/D screw-action mechanical testing system, using a crosshead speed of 1 mm min^{-1}.

3. RESULTS AND DISCUSSION

3.1 *Fiber properties*

Figure 4(a) and 4(b) show SEM photographs of as-received and ozone treated fibers. The surface morphology and diameter (15 ± 3 mm) of the fiber were not changed by the ozone treatment. The specific surface area could not be determined, using the Micromeritics ASAP 2010 analyzer, due to volatile evolution during evacuation. Therefore, we have no evidence for an increase in specific surface area after the ozone treatment. Nevertheless, it is likely that an increase in specific surface area occurred.

The surface oxygen concentration was increased from 13.5 to 24.0 at% after ozone treatment, as shown by O_{1s} and C_{1s} peaks in ESCA. As a result, the surface hydrogen concentration was decreased from 86.5 to 76.0 at%. As shown in Table 2, ozone treatment also changed the surface oxygen from C–O configuration to C=O configuration. The latter configuration is known to be more chemically active than the former configuration.

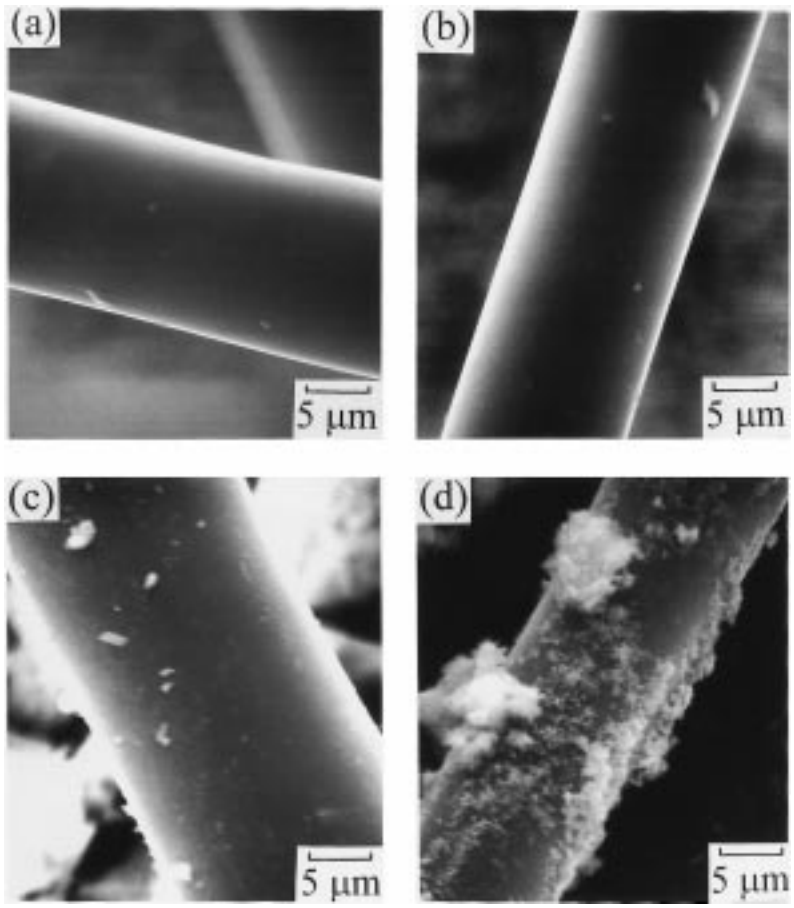

Fig. 4. SEM photographs of single carbon fiber: (a) as-received, (b) ozone treated. SEM photographs of single carbon fiber after pull-out testing: (c) as-received, (d) ozone treated.

Table 2. Fractions of surface carbon atoms bonded as C–H, C–O and C=O

	C–H (%)	C–O (%)	C=O (%)
As-received	86.5	13.5	0
After O_3 exposure	76.0	0	24.0

Table 3. Contact angle ($\pm 1^\circ$) between carbon fiber and water

Fiber		Advancing	Receding
As-received	1st cycle	86.1	30.2
	2nd cycle	84.9	28.5
	3rd cycle	83.2	28.3
	Average	84.7	29.0
NaOH treated	1st cycle	40.6	0
	2nd cycle	38.8	0
	3rd cycle	37.6	0
	Average	39.0	0
HNO_3 treated	1st cycle	35.1	0
	2nd cycle	32.5	0
	3rd cycle	28.4	0
	Average	32.0	0
O_3 treated	1st cycle	0	0
	2nd cycle	0	0
	3rd cycle	0	0
	Average	0	0

Both tensile strength and volume electrical resistivity were not affected by the ozone treatment. This is consistent with the absence of a surface morphological change.

The advancing and receding contact angles for the first three cycles of advancing (increasing immersion depth) and receding (decreasing immersion depth) are shown in Table 3 for each of the as-received, NaOH treated, HNO_3 treated and ozone treated fibers. The plots of wetting force per unit length of fiber vs immersion depth are shown in Fig. 5 for the ozone treated fiber. The receding angle was decreased to zero by any of these three treatments. The advancing angle was decreased to zero only for the ozone treated fiber, though it was still substantially decreased for the NaOH and HNO_3 treated fibers. The advancing angle decreased in the order: (i) as-received, (ii) NaOH treated, (iii) HNO_3 treated and (iv) O_3 treated fibers. The improved wetting is presumably due to the oxygen-containing functional groups on the fiber surface resulting from the ozone or HNO_3 treatment. As cement paste is a hydraulic mix, the improved wetting of the fiber by water

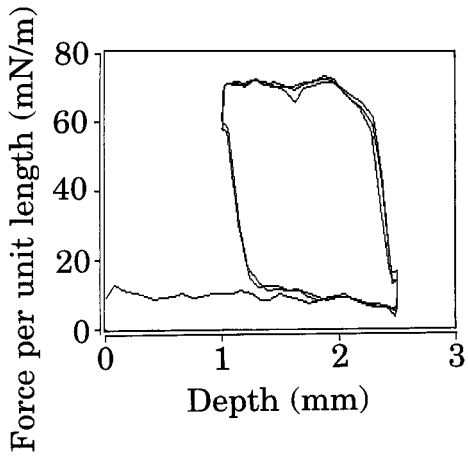

Fig. 5. Plot of wetting force per unit length of fiber vs immersion depth in the first three advancing (low force) and receding (high force) cycles for ozone treated fiber.

means improved wetting of the fiber by the cement paste.

Figure 6 shows the correlation of the contact resistivity and the bond strength for plain cement paste in contact with six different types of fibers (as-received and five types of treated fibers). Among the samples in each case, a high bond strength is associated with a low contact resistivity, because a high bond strength is associated with a low content of interfacial voids, which are electrically insulating. This trend within each case is consistent with that in ref. [40].

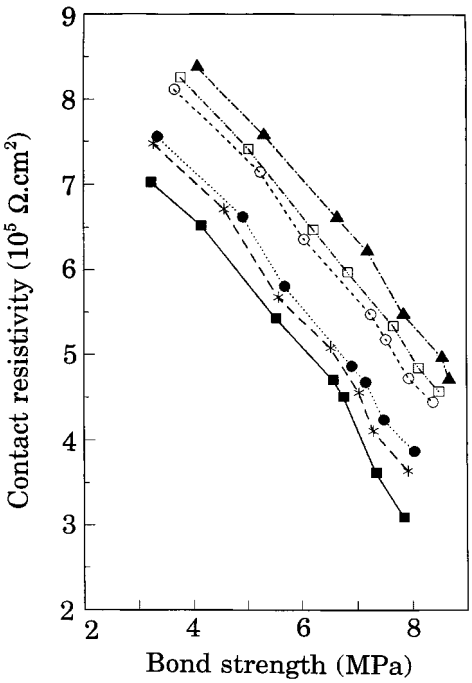

Fig. 6. Variation of contact electrical resistivity with bond strength for plain cement in contact with as-received (■) and five types of treated carbon fibers: acetic acid (*), H_2O_2 (●), NaOH (○), nitric acid (□) and O_3 (▲).

Comparison among the curves in Fig. 6 shows that all treatments increased both bond strength and contact resistivity, such that the magnitude of either effect increased in the order: acetic acid, H_2O_2, NaOH, nitric acid and O_3. Both effects are mainly attributed to the formation of an interfacial layer of high volume resistivity due to the treatment. This interfacial layer enhances the bonding and increases the contact resistivity. For the oxidizing chemicals, such as acetic acid, H_2O_2, nitric acid and O_3, the interfacial layer is believed to be oxygen-containing functional groups [41], which help the wettability of the fibers by the cement. Among the chemicals used, ozone (O_3) is the most oxidizing chemical and nitric acid is the second most oxidizing chemical, so O_3 gave the largest effects while nitric acid gave the second largest effects. The trend in Fig. 6 is consistent with that in Table 3, so that a high bond strength is associated with a low advancing contact angle.

Figure 4(c) and 4(d) show SEM photographs of a single fiber after pull-out from the cement paste. The amount of adherent after pull-out was larger for the ozone treated fiber than the as-received fiber. This is consistent with the greater bond strength after ozone treatment (Fig. 6).

3.2 *Composite properties*

Table 4 shows the effect of ozone treatment of the carbon fiber on the tensile properties of cement pastes. Ozone treatment increased the tensile strength, modulus and ductility for all four formulations of carbon fiber reinforced cement paste, except that the treatment decreased the ductility for the formulation with latex (due to the high fiber–matrix bond strength for the latex case, even without the fiber treatment [35]). The fractional increase in tensile strength due to the fiber treatment was particularly large (38%) for the formulation with methylcellulose (but no silica fume). The fractional increase in tensile modulus due to the fiber treatment was particularly large (82%) for the formulation with latex. The fractional increase in tensile ductility due to the fiber treatment was particularly large (26%) for the formulation with methylcellulose and silica fume. With the fiber treatment, the highest tensile strength reached was 3.42 MPa (with latex), the highest tensile modulus reached was 18.2 GPa (with methylcellulose and silica fume) and the highest tensile ductility reached was 0.0413% (with latex).

The volume electrical resistivity at 28 days of curing was 3.62×103 and 3.27×103 V · cm for mortars with as-received and ozone treated fibers, respectively. Even though ozone treatment increased the contact resistivity between fiber and cement paste (Fig. 6), it decreased the volume resistivity of the mortar. This means that the ozone treatment improved the dispersion of fibers in the mortar.

Figure 7 shows the variation of the drying shrinkage with curing time up to 40 days for (a) plain mortar (data from ref. [42]), (b) mortar with methyl-

Table 4. Effect of ozone treatment of carbon fiber on tensile properties of carbon fiber (0.51 vol%) reinforced cement paste at 28 days

	+F	+F+M	+F+M+SF	+F+L
Strength (MPa)*				
Without treatment	1.36 (±1.2%)	2.01 (±3.2%)	1.97 (±5.1%)	3.18 (±3.1%)
With treatment	1.58 (±3.8%)	2.78 (±3.2%)	2.23 (±2.7%)	3.42 (±3.1%)
Modulus (GPa)†				
Without treatment	9.4 (±1.2%)	10.3 (±2.1%)	13.8 (±2.6%)	7.6 (±2.1%)
With treatment	10.3 (±3.4%)	12.7 (±2.0%)	18.2 (±2.1%)	13.8 (±2.4%)
Ductility (%)‡				
Without treatment	0.0121 (±3.1%)	0.0198 (±1.1%)	0.0167 (±2.6%)	0.0462 (±1.9%)
With treatment	0.0140 (±2.2%)	0.0231 (±1.8%)	0.0211 (±2.1%)	0.0413 (±1.7%)

Note: F = fiber, M = methylcellulose, SF = silica fume, L = latex.
*Strength = 0.91 MPa (±2.7%) for plain cement paste (without fibers).
†Modulus = 11.2 GPa (±2.1%) for plain cement paste (without fibers).
‡Ductility = 0.0041 (±1.9%) for plain cement paste (without fibers).

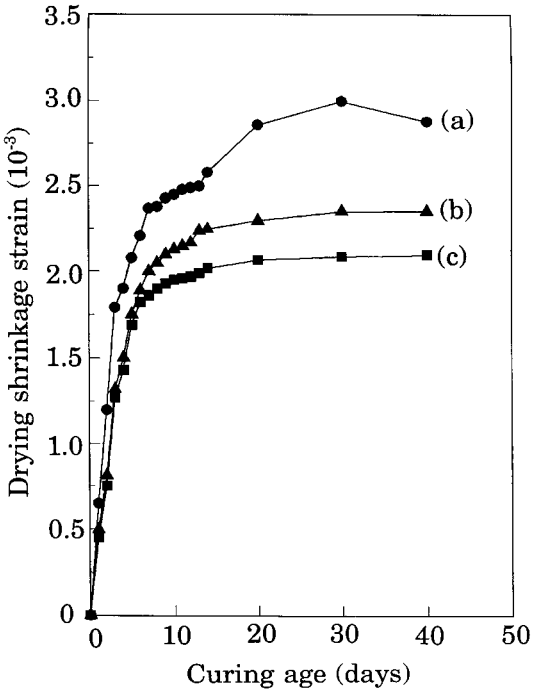

Fig. 7. Plot for drying shrinkage strain vs curing age for (a) plain mortar, (b) mortar with methylcellulose, silica fume and as-received fibers, and (c) mortar with methylcellulose, silica fume and ozone treated fibers.

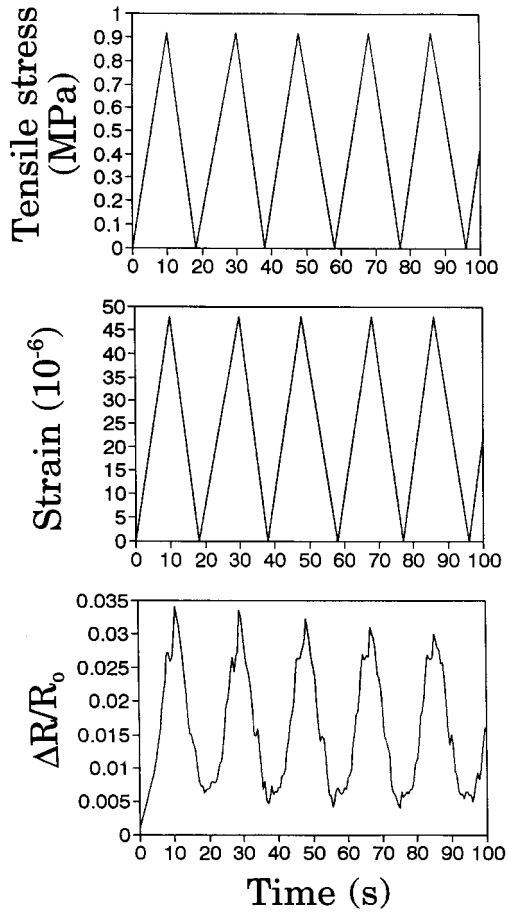

Fig. 8. DR/R_0, strain and stress during cyclic tensile loading of cement paste with as-received fibers at 28 days of curing.

cellulose, silica fume and as-received fibers, and (c) mortar with methylcellulose, silica fume and ozone treated fibers. The drying shrinkage of (b) was less than that of (a), as previously reported [42]; that of (c) was less than that of (b), indicating that ozone treatment increased the effectiveness of the fibers in reducing the drying shrinkage.

Figure 8 gives the fractional DC resistance increase (DR/R_0) during first tensile loading of cement paste with 0.51 vol% as-received carbon fibers at a stress amplitude of 0.9 MPa, or a strain amplitude of 4.8×10^{-5}, which was within the elastic regime, at 28 days of curing. (The tensile strength was 1.97 MPa.) The resistance was in the stress direction. Both stress and strain returned to zero at the end of each cycle. The DR/R_0 value increased during tensile loading in each cycle and decreased during unloading in each cycle, with a gage factor (fractional change in resistance per unit strain) of 625. This is due to fiber pull-out during loading and fiber push-in during unloading, as explained in refs. [20–23]. At the end of the first cycle, DR/R_0 was positive rather than zero. This

resistance increase is attributed to damage of the fiber–cement interface due to the fiber pull-out and push-in. As cycling progressed, both the maximum $D R/R_0$ and minimum $D R/R_0$ values in a cycle decreased. This is attributed to damage of the cement matrix separating adjacent fibers at their junction; this damage increased the chance for adjacent fibers to touch one another, thereby decreasing the resistivity.

Figure 9 shows results similar to Fig. 8, but for ozone treated fibers instead of as-received fibers. The main difference between Figs. 9 and 8 is that the downward trend in $D R/R_0$ in Fig. 8 is absent in Fig. 9. This is due to the superior mechanical properties of the cement paste with ozone treated fibers compared to those of the cement paste with as-received fibers (Table 4). The gage factor is 700 from Fig. 9—higher than the value of 625 from Fig. 8 for as-received fibers. Thus, ozone treatment of the fibers resulted in improvement of the strain sensing ability in two ways, i.e. increase in gage factor and better repeatability upon repeated loading.

Figure 10 gives $D R/R_0$ values during first cyclic compressive loading of mortar with 0.24 vol% as-received carbon fibers at a stress amplitude of 16 MPa, or a strain amplitude of $8 \times 10^{-}4$, which was within the elastic regime, at 28 days of curing. (The compressive strength was 45 MPa.) The resistance was in the stress direction. Both stress and strain returned to zero at the end of each cycle. The $D R/R_0$ value decreased during compressive loading in each cycle and increased during unloading in each cycle, with a gage factor of 500. This is due to fiber push-in during loading and fiber pull-out during unloading. At the end of the first cycle, $D R/R_0$ was positive rather than zero. This resistance increase is attributed to damage of the fiber–cement interface due to the fiber push-in and pull-out. As cycling progressed, both the maximum $D R/R_0$ and minimum $D R/R_0$ values in a cycle decreased. This is attributed to damage of the cement matrix separating adjacent fibers at their junction, as explained above. This decrease from cycle to cycle persisted for the first ~150 cycles, after which the maximum and minimum $D R/R_0$ values did not change with cycling.

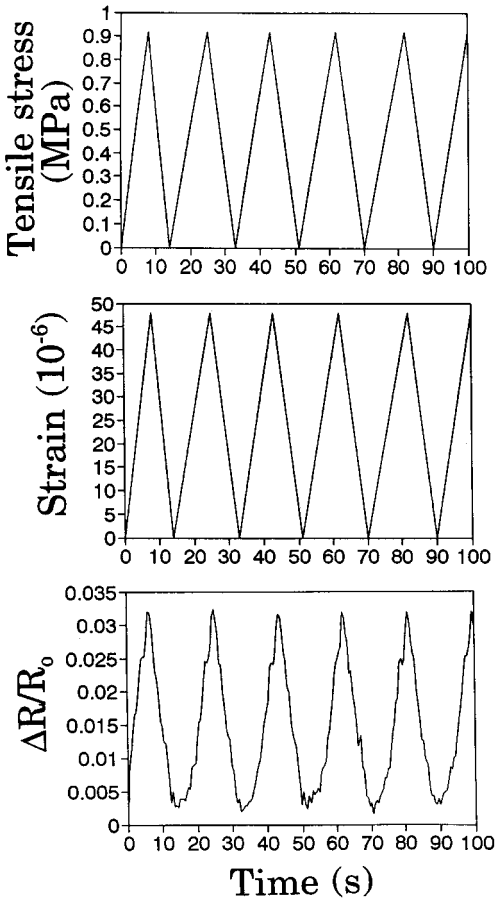

Fig. 9. $D R/R_0$, strain and stress during cyclic tensile loading of cement paste with ozone treated fibers at 28 days of curing.

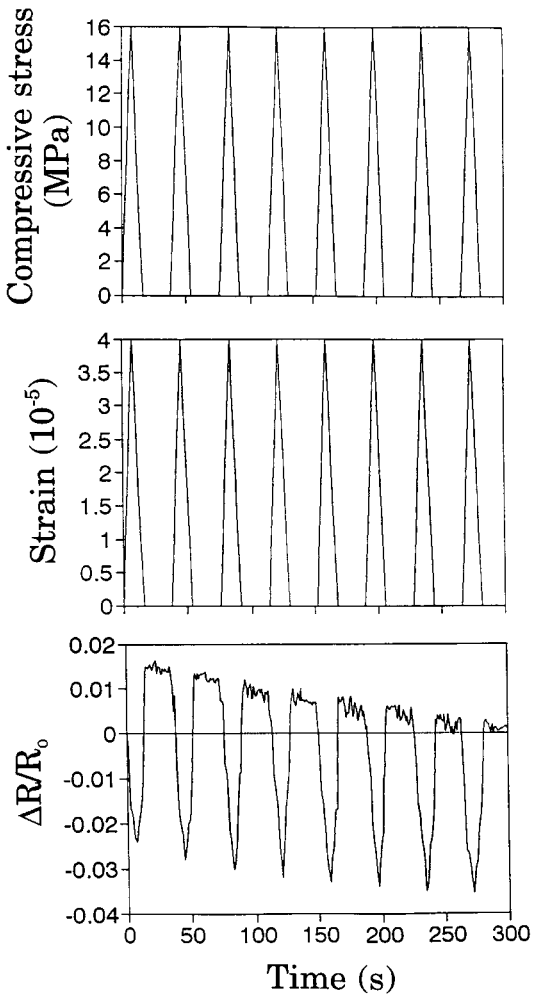

Fig. 10. $D R/R_0$, strain and stress during cyclic compressive loading of mortar with as-received fibers at 28 days of curing.

Figure 11 shows results similar to Fig. 10, but for ozone treated fibers instead of as-received fibers. Note the absence of a constant strain period during each strain cycle in Fig. 11, but the presence of this period in Fig. 10. The main difference between Figs. 11 and 10 is that the downward trend in DR/R_0 values in Fig. 10 is absent in Fig. 11. This is due to the superior mechanical properties of the mortar with ozone treated fibers compared to those of the mortar with as-received fibers, as suggested by the data in Table 4 for cement pastes. The gage factor is 560 from Fig. 11—higher than the value of 500 from Fig. 10 for as-received fibers. Thus, ozone treatment of the carbon fibers resulted in improvement of the strain sensing ability, whether under tension or compression. The improved repeatability obtained by ozone treatment is similar to that obtained by decreasing the curing age to seven days [43], as both ozone treatment and curing age decrease increased the fiber–matrix bond strength.

The gage factor of a conventional resistive strain gage is around 2. The gage factors reported here are exceptionally high.

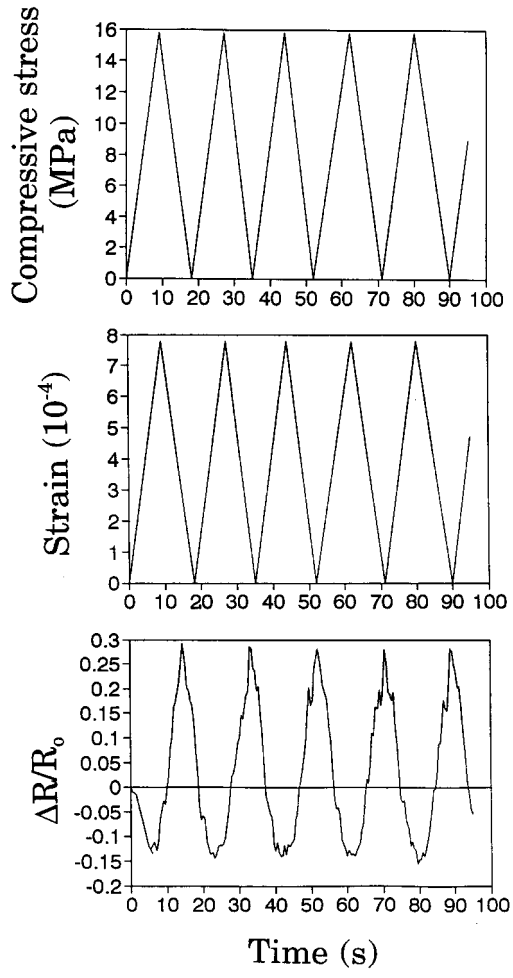

Fig. 11. DR/R_0, strain and stress during first cyclic compressive loading of mortar with ozone treated fibers at 28 days of curing.

4. CONCLUSION

Ozone treatment of isotropic-pitch-based carbon fiber was found to increase the surface oxygen concentration and change the surface oxygen from C–O to C=O configurations, thereby causing the contact angle between fiber and water to be decreased to zero and increasing the contact electrical resistivity between fiber and cement paste. As a consequence of the improved wettability, the bond strength between fiber and cement paste was increased, thereby causing the tensile strength, modulus and ductility of carbon fiber reinforced cement paste to increase. Moreover, the fiber dispersion in mortar was improved, as indicated by decrease in volume resistivity of the mortar. In addition, the effectiveness of the fibers in reducing the drying shrinkage was improved. As a result of the improved mechanical properties and fiber dispersion, the strain sensing ability of carbon fiber reinforced mortar was improved in terms of increased gage factor and better repeatability upon repeated loading. The ozone treatment did not affect the morphology, tensile strength or volume electrical resistivity of the fiber itself. Ozone treatment was more effective than treatments involving nitric acid, NaOH, H_2O_2 and acetic acid in increasing the bond strength between fiber and cement paste.

Acknowledgements—This work was supported by the National Science Foundation.

REFERENCES

1. Chen, P. and Chung, D. D. L., *ACI Mater. J.*, 1996, **93**(2), 129.
2. Chen, P. and Chung, D. D. L., *Composites*: *Part B*, 1996, **27B,** 269.
3. Yang, X. and Chung, D. D. L., *Composites*, 1992, **23**(6), 453.
4. Banthia, N., Djeridane, S. and Pigeon, M., *Cem. Concr. Res.*, 1992, **22,** 804.
5. Banthia, N., Moncef, A., Chokri, K. and Sheng, J., *Can. J. Civ. Eng.*, 1994, **21,** 999.
6. Li, V. C. and Obla, K. H., *Composites Eng.*, 1994, **4**(9), 947.
7. Katz, A. and Bentur, A., *Cem. Concr. Res.*, 1993, **24**(2), 214.
8. Katz, A. and Bentur, A., *Cem. Concr. Composites*, 1995, **17,** 87.
9. Katz, A., Li, V. C. and Kazmer, A., *J. Mater. Civ. Eng.*, May 1995, 125–128.
10. Nakagawa, H., Akihama, S., Suenaga, T., Taniguchi, Y. and Yoda, K., *Adv. Composite Mater.*, 1993, **3**(2), 123.
11. Park, S. B., Lee, B. I. and Lim, Y. S., *Cem. Concr. Res.*, 1991, **21**(4), 589.
12. Park, S. B. and Lee, B. I., *Cem. Concr. Composites*, 1993, **15**(3), 153.
13. Sakai, H., Takahashi, K., Mitsui, Y., Ando, T., Awata, M. and Hoshijima, T., *Fiber Reinforced Concrete*, ACI SP-142, ed. J. I. Daniel and S. P. Shah. ACI, Detroit, MI, 1994, pp. 121–140.

14. Soroushian, P., Aouadi, F. and Nagi, M., *ACI Mater. J.*, 1991, **88**(1), 11.
15. Soroushian, P., Nagi, M. and Okwuegbu, A., *ACI Mater. J.*, 1992, **89**(5), 491.
16. Soroushian, P., Nagi, M. and Hsu, J., *ACI Mater. J.*, 1992, **89**(3), 267.
17. Toutanji, H. A., El-Korchi, T., Katz, R. N. and Leatherman, G. L., *Cem. Concr. Res.*, 1993, **23,** 618.
18. Toutanji, H. A., El-Korchi, T. and Katz, R. N., *Cem. Concr. Composites*, 1994, **16,** 15.
19. Zayat, K. and Bayasi, Z., *ACI Mater. J.*, 1996, **93,** 178.
20. Chen, P. and Chung, D. D. L., *Smart Mater. Struct.*, 1993, **2,** 22.
21. Chen, P. and Chung, D. D. L., *J. Am. Ceram. Soc.*, 1995, **78,** 816.
22. Chen, P. and Chung, D. D. L., *Composites*: *Part B*, 1996, **27B,** 11.
23. Chen, P. and Chung, D. D. L., *ACI Mater. J.*, 1996, **93**(4), 341.
24. Fu, X. and Chung, D. D. L., *Cem. Concr. Res.*, 1996, **26**(1), 15.
25. Fu, X., Ma, E., Chung, D. D. L. and Anderson, W. A., *Cem. Concr. Res.*, 1997, **27**(6), 845.
26. Fitzer, E. and Heine, M., in *Composite Materials Series, Vol. 2, Fibre Reinforced Composite Materials*, ed. A. R. Bunsell. Elsevier, Amsterdam, 1988, pp. 73–148.
27. Wright, W. W., *Compos. Polym.*, 1990, **3**(4), 231.
28. Allred, R. E. and Harrah, L. A., in *Proc. Int. SAMPE Symp. and Exhib., 34, Tomorrow's Materials: Today*, ed. G. A. Zakrzewski, D. Mazenko, S. T. Peters and C. D. Dean, 1989, pp. 2559–2568.
29. Yip, P. W. and Lin, S. S., in *Mater. Res. Soc. Symp. Proc., Vol. 170, Interfaces Compos.*, ed. C. G. Pantano and E. J. H. Chen, 1990, pp. 339–344.
30. Chang, T. C. and Jang, B. Z., in *Mater. Res. Soc. Symp. Proc., Vol. 170, Interfaces Compos.*, ed. C. G. Pantano and E. J. H. Chen, 1990, pp. 321–326.
31. King, T. R., Adams, D. F. and Buttry, D. A., *Composites*, 1991, **22**(5), 380.
32. Rich, M. J. and Drzal, L. T., *J. Reinf. Plast. Compos.*, 1988, **7**(2), 145.
33. Drzal, L. T., *Vacuum*, 1997, **41,** (7–9), 1615.
34. *Adhesion and Bonding in Composites*, ed. R. Yosomiya, K. Morimoto, A. Nakajima, Y. Ikada and T. Suzuki. Marcel Dekker, New York, 1990, pp. 257–281 (chapter on Interfacial Effect of Carbon-Fiber-Reinforced Composite Material).
35. Fu, X., Lu, W. and Chung, D. D. L., *Cem. Concr. Res.*, 1996, **26**(7), 1007.
36. Fu, X., Lu, W. and Chung, D. D. L., *Cem. Concr. Res.*, 1996, **26**(10), 1485.
37. Krekel, G., Hüttinger, K. J., Hoffman, W. P. and Silver, D. S., *J. Mater. Sci.*, 1994, **29**(11), 2968.
38. Chen, P., Fu, X. and Chung, D. D. L., *ACI Mater. J.*, 1997, **94**(2), 147.
39. Chen, P. and Chung, D. D. L., *J. Electron. Mater.*, 1995, **24**(1), 47.
40. Fu, X. and Chung, D. D. L., *Cem. Concr. Res.*, 1995, **25**(7), 1391.
41. Chiang, H.-L., Chiang, P. C. and You, J. H., *Toxicological Environ. Chem.*, 1995, **47,** (1–2), 97.
42. Chen, P. and Chung, D. D. L., *Composites*, 1993, **24**(1), 33.
43. Fu, X. and Chung, D. D. L., *Cem. Concr. Res.*, 1997, **27**(9), 1313.